AGU PUBLICATIONS

Geophysical Research Letters

RESEARCH LETTER
10.1002/2014GL059250

Key Points:
- Groundwater flux is major component of the hydrologic budget of ice streams
- Groundwater flux lubricates fast ice streaming motion
- Groundwater flux brings nutrients to subglacial lakes

Supporting Information:
- Readme
- Table S1
- Text S1
- Figure S1
- Figure S2

Correspondence to:
P. Christoffersen,
pc350@cam.ac.uk

Citation:
Christoffersen, P., M. Bougamont, S. P. Carter, H. A. Fricker, and S. Tulaczyk (2014), Significant groundwater contribution to Antarctic ice streams hydrologic budget, *Geophys. Res. Lett.*, *41*, 2003–2010, doi:10.1002/2014GL059250.

Received 10 JAN 2014
Accepted 27 FEB 2014
Accepted article online 3 March 2014
Published online 26 MAR 2014

Significant groundwater contribution to Antarctic ice streams hydrologic budget

Poul Christoffersen[1], Marion Bougamont[1], Sasha P. Carter[2], Helen A. Fricker[2], and Slawek Tulaczyk[3]

[1]Scott Polar Research Institute, University of Cambridge, Cambridge, UK, [2]Institute of Geophysics and Planetary Physics, Scripps Institution of Oceanography, University of California, San Diego, California, USA, [3]Department of Earth and Planetary Sciences, University of California, Santa Cruz, California, USA

Abstract Satellite observations have revealed active hydrologic systems beneath Antarctic ice streams, but sources and sinks of water within these systems are uncertain. Here we use numerical simulations of ice streams to estimate the generation, flux, and budget of water beneath five ice streams on the Siple Coast. We estimate that 47% of the total hydrologic input (0.98 $km^3\,yr^{-1}$) to Whillans (WIS), Mercer (MIS), and Kamb (KIS) ice streams comes from the ice sheet interior and that only 8% forms by local basal melting. The remaining 45% comes from a groundwater reservoir, an overlooked source in which depletion significantly exceeds recharge. Of the total input to Bindschadler (BIS) and MacAyeal (MacIS) ice streams (0.56 $km^3\,yr^{-1}$), 72% comes from the interior, 19% from groundwater, and 9% from local melting. This contrasting hydrologic setting modulates the ice streams flow and has important implications for the search for life in subglacial lakes.

1. Introduction

Discharge of ice from the Antarctic ice sheet is governed by ice streams, which are fast flowing arteries, tens of kilometers wide, several-hundred-kilometers long, and responsible for nearly all of the Antarctic contribution to sea level rise [*Rignot et al.*, 2008; *Shepherd et al.*, 2012]. Studies have shown that the fast flow of ice streams (~500 m yr^{-1} or higher) is facilitated by weak subglacial sediment [*Blankenship et al.*, 1986], which provides little frictional resistance [*Kamb*, 1991]. Although geophysical surveys indicate that this type of subglacial sediment is widespread [*Blankenship et al.*, 1986; *Rooney et al.*, 1987; *Smith*, 1997], so far this has only been directly observed at the Siple Coast, where samples collected in boreholes confirmed it to be till [*Engelhardt et al.*, 1990], a glacially produced material with highly non-linear rheology [*Kamb*, 1991; *Tulaczyk et al.*, 2000a]. The incorporation of non-linear till rheology in numerical ice sheet models has provided key new insights to the dynamics of ice streams [*Bougamont et al.*, 2011], explaining, e.g., their semi-periodic stagnation and reactivation on the Siple Coast [*Hulbe and Fahnestock*, 2007; *Catania et al.*, 2012]. Less certain, however, is the effect of water flowing between interconnected subglacial lakes and along the ice stream beds [*Gray et al.*, 2005; *Fricker et al.*, 2007; *Carter and Fricker*, 2012].

This work uses a higher-order ice flow model constrained by Bedmap2 ice thickness and bedrock geometry [*Fretwell et al.*, 2013] to reproduce flow and basal conditions for ice streams on the Siple Coast. Using a numerical inversion technique, we convert surface velocities observed in 1997 [*Joughin et al.*, 2002] and 2009 [*Rignot et al.*, 2011] into two independently derived maps of basal traction. The latter are combined with the Coulomb plastic till rheology [*Tulaczyk et al.,* 2000a, 2000b] in order to estimate shear strength and storage of water in the till. By routing water at the bed, we obtain hydrologic pathways that connect observed locations of subglacial lakes. We complete the analysis by quantifying the hydrologic budget for each ice stream based on (1) water produced and consumed by basal melting and freezing, (2) water entering and leaving the subglacial till layer, and (3) flow of water along the ice-till interface. While the contribution from (1) is similar for all ice streams, the contributions from (2) and (3) differ markedly, with high groundwater fluxes at MIS, WIS, and KIS, while BIS and MacIS are influenced predominantly by a large supply of water from the ice sheet interior.

2. Methods

2.1. Ice Flow Model

In this work we use the higher-order Community Ice Sheet Model (CISM) [*Bougamont et al.*, 2011; *Price et al.*, 2011; *Bindschadler et al.*, 2013] to simulate flow of ice streams on the Siple Coast of Antarctica. The model solves the

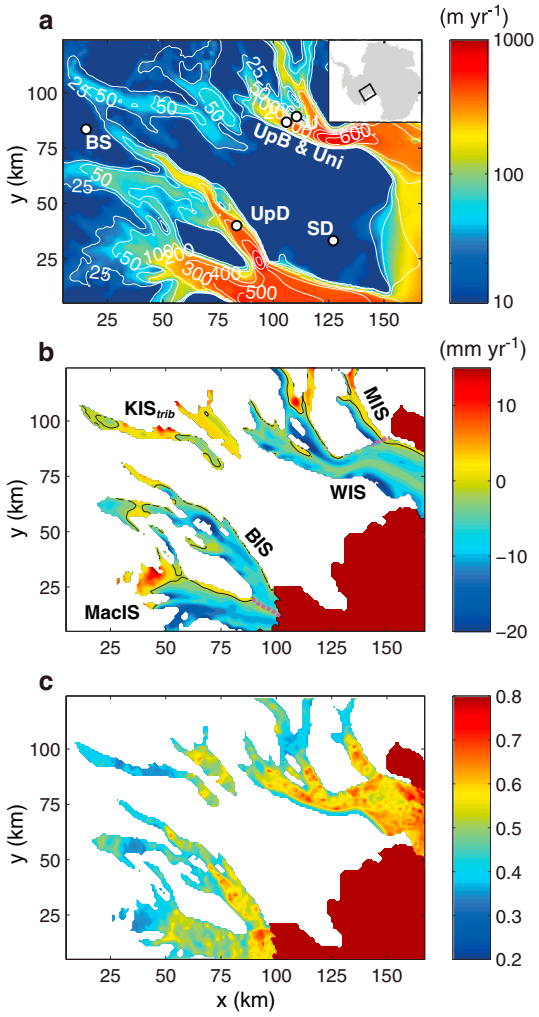

Figure 1. (a) Surface velocity (m yr^{-1}) of ice streams on the Siple Coast, as observed by satellite in 2009 (color scale) and reproduced with CISM (white contours). White dots show locations of borehole drill sites referred to in text (UpB: UpB camp; Uni: Unicorn; BS: Byrd station; SD: Siple Dome; UpD: UpD camp). Inset shows location of study area. (b) Modeled rates of basal melting and freezing (mm yr^{-1}) beneath MIS, WIS, KIS$_{trib}$, BIS, and MacIS, when model reproduces surface velocities shown in Figure 1a. Solid black lines show the zero contour. Dashed magenta lines denote boundaries between MIS and WIS and between BIS and MacIS. Dark red area is the Ross Ice Shelf, where ice is no longer in contact with the bed. (c) Till void ratios (dimensionless) calculated from basal traction values, when model reproduces surface velocities shown in Figure 1a. Axes (*x*,*y*) show distance (km) in a polar stereographic grid with reference to 76.727°S and 141.53°W.

conservation of momentum, mass, and thermal energy, as described in *Bougamont et al.* [2011], and is applied with a 5 km spatial resolution. We define the extent of MIS, WIS, KIS, BIS, and MacIS according to the area covering their fast flowing trunks as well as the tributaries that feed them (Figure 1a). The latter are specified by surface velocity of 50–200 m yr^{-1}, while trunks are defined by surface velocity >200 m yr^{-1}. The study of KIS is limited to its tributaries (henceforth KIS$_{trib}$) because its trunk is stagnant (ice flow <10 m yr^{-1}).

To obtain realistic flow in the model, we use an inversion technique by which surface velocity is iterated [as explained in *Price et al.*, 2011] toward values observed in (A) 1997 [*Joughin et al.*, 2002] and (B) 2009 [*Rignot et al.*, 2011]. With constant model geometry [*Fretwell et al.*, 2013], climate [*Arthern et al.*, 2006; *Comiso*, 2000], and geothermal heat flux [*Maule et al.*, 2005; *Shapiro and Ritzwoller*, 2004], we converge ice temperature, effective viscosity, and velocity fields to an equilibrium in which basal sliding and internal ice deformation together reproduce the observed surface velocity (see Text S1 in Auxiliary Materials).

2.2. Basal Thermal Regime

Rates of basal melting $\dot{m}$ (negative for freezing) are calculated from the basal heat budget:

$$\dot{m} = \frac{\tau_b U_b + G - k\theta_b}{\rho L} \quad (1)$$

where τ_b and U_b are basal traction and sliding velocity, which collectively comprise frictional heat; G is geothermal heat flux; k and θ_b are thermal conductivity of ice and vertical basal ice temperature gradient, which yield the conductive heat loss; ρ is ice density; and L is specific latent heat of fusion.

2.3. Till Properties

Basal traction values obtained from the two model inversions are used to estimate till shear strength and the corresponding till void ratio. The latter is a property directly related to porosity and defined as the volumetric ratio of pores and solids in the till layer. This analysis is based on two specific till rheological characteristics, both established from laboratory analysis of samples collected from beneath the ice streams [*Tulaczyk et al.*, 2000a]. The first is that till shear strength, τ_f, is a linear function of the effective normal stress, N, i.e., the stress exerted by the direct contact between solid particles. Henceforth, $\tau_f \propto f N$ where $f = \tan\phi$ is a constant defined by the friction angle of the till, which is 24 ± 0.3° [*Tulaczyk et al.*, 2000a]. The second characteristic is that till compressibility can be described by a logarithmic function relating the till void ratio, e, to the effective normal stress. Thus, $e \propto C \ln(N)$ where C is the constant of compressibility, which has a relatively narrow range of values (0.12–0.15) when the till is normally consolidated. We exclude

Table 1. Hydrologic Budgets for West Antarctic Ice Streams

Hydrologic Budget		Ice		Till		Basal Water System	
Ice Stream	Area[a] km^2	Melt[b] $km^3\ yr^{-1}$	Freeze[b] $km^3\ yr^{-1}$	Water Out[c] $km^3\ yr^{-1}$	Water In[c] $km^3\ yr^{-1}$	Inflow[d] $km^3\ yr^{-1}$	Outflow[d] $km^3\ yr^{-1}$
MIS	7,000	0.01 (0.01)	−0.02 (−0.03)	0.03 ± 0.01	−0.01 ± 0.00	0.11	−0.12
WIS	43,000	0.02 (0.03)	−0.23 (−0.23)	0.35 ± 0.11	−0.09 ± 0.03	0.35	−0.43
KIS_{trib}	14,000	0.04 (0.02)	−0.00 (−0.02)	0.05 ± 0.02	−0.07 ± 0.02		
BIS	25,000	0.01 (0.00)	−0.12 (−0.15)	0.05 ± 0.02	−0.05 ± 0.02	0.20	−0.09
MacIS	30,000	0.04 (0.03)	−0.15 (−0.18)	0.06 ± 0.02	−0.04 ± 0.01	0.21	−0.10
Sum		0.13 (0.09)	−0.53 (−0.61)	0.55 ± 0.16	−0.27 ± 0.08	0.86	−0.74

[a]Area of each ice stream including trunk and tributaries.
[b]Melt (>0) and freeze (<0) are the annual volumes of water, produced by basal melting and consumed by basal freezing. The uncertainty is small (±6%) due to good agreement between model and observations. Numbers in brackets are based on satellite magnetic geothermal heat flux values, not used in analysis because they underestimate geothermal heat flow at KIS_{trib}, BIS, and MacIS.
[c]Water out (>0) and water in (<0) are the annual volumes of water flowing out of and into the till layer. The uncertainty is ±30% due to variation in till layer thickness.
[d]Inflow (>0) and outflow (<0) are the annual volumes of water entering and leaving each ice stream laterally via a regional basal water system.

significant over-consolidation as a possibility given the observed weak and highly porous state of the till [*Tulaczyk et al.*, 2000a, 2001]. Combining the two relations in an empirical format yields $e = -\ln(\tau_f/a)/b$ where $a = 944 \times 10^6$ Pa and $b = 21.7$ are previously established constants [*Tulaczyk et al.*, 2000b]. We expect errors from using these rheological parameters over a wide region to be small because the till is known to be regionally homogeneous [*Kamb*, 2001]. The assumed Coulomb plastic till rheology [*Tulaczyk et al.*, 2000a] is widely accepted [*Clarke*, 2005], and supported by similar rheological properties of tills found in a variety of other glacial settings [*Clarke*, 1987; *Hooke et al.*, 1997; *Iverson et al.*, 1998; *Rathbun et al.*, 2008].

2.4. Subglacial Hydrology

To constrain the flow of water along the ice stream beds, we use the hydrological model included in CISM. This model component directs water down the hydraulic potential surface using a steady-state directional routing algorithm, where cells with lower hydraulic potential receive a fraction of the outflow, depending on the slope of the hydraulic potential surface. The hydrological model is identical to the one used previously to study subglacial hydrology at the Siple Coast [*Carter and Fricker*, 2012; *Carter et al.*, 2013].

3. Results

3.1. Basal Melting and Freezing

The modeled distribution of basal melting and freezing, when the model reproduces flow as observed in 2009, is shown in Figure 1b. The net basal meltwater production is −0.01, −0.21, +0.04, −0.11, and −0.11 $km^3\ yr^{-1}$ for MIS, WIS, KIS_{trib}, BIS, and MacIS, respectively (Table 1). The frictional heat term in equation (1) is captured well in our model because flow is iterated toward observed surface velocities with an average misfit of just 6 m yr^{-1} (Figure 1a), which is small relative to the average magnitude of flow (187 m yr^{-1}). Flow in the modeled ice streams occurs predominantly by sliding at the bed, which is consistent with in situ measurements in a borehole [*Engelhardt and Kamb*, 1998]. When basal traction in our model is converted to till shear strength, we obtain values in good agreement with observations. We estimate the shear strength of till beneath the trunk of WIS to average 5 kPa, which is within range of measurements made at this location (0.02–7.9 kPa [*Kamb*, 2001]). Overall, we estimate the error of the frictional heat term to be less than 10%.

The conductive heat loss at the ice stream beds is proportional to the basal ice temperature gradient (equation (1)). We thus compare the modeled basal temperature gradients at locations where such gradients have been measured [*Engelhardt*, 2004], including UpB camp and Unicorn on WIS, Siple Dome between KIS and BIS, Byrd Station, and UpD camp on BIS (Figure 1a). We exclude measurements from UpC camp on KIS trunk because ice temperature at this site has not equilibrated to stagnation of flow 170 years ago [*Joughin et al.*, 2002]. For the other drill sites, our model predicts basal ice temperature gradients, which are either within range (UpB, Byrd, and Unicorn) or close to (Siple Dome and UpD) measured values (Table S1). The overall error between modeled and observed temperature gradients averages just 6%, which shows that our model captures the conductive heat loss well.

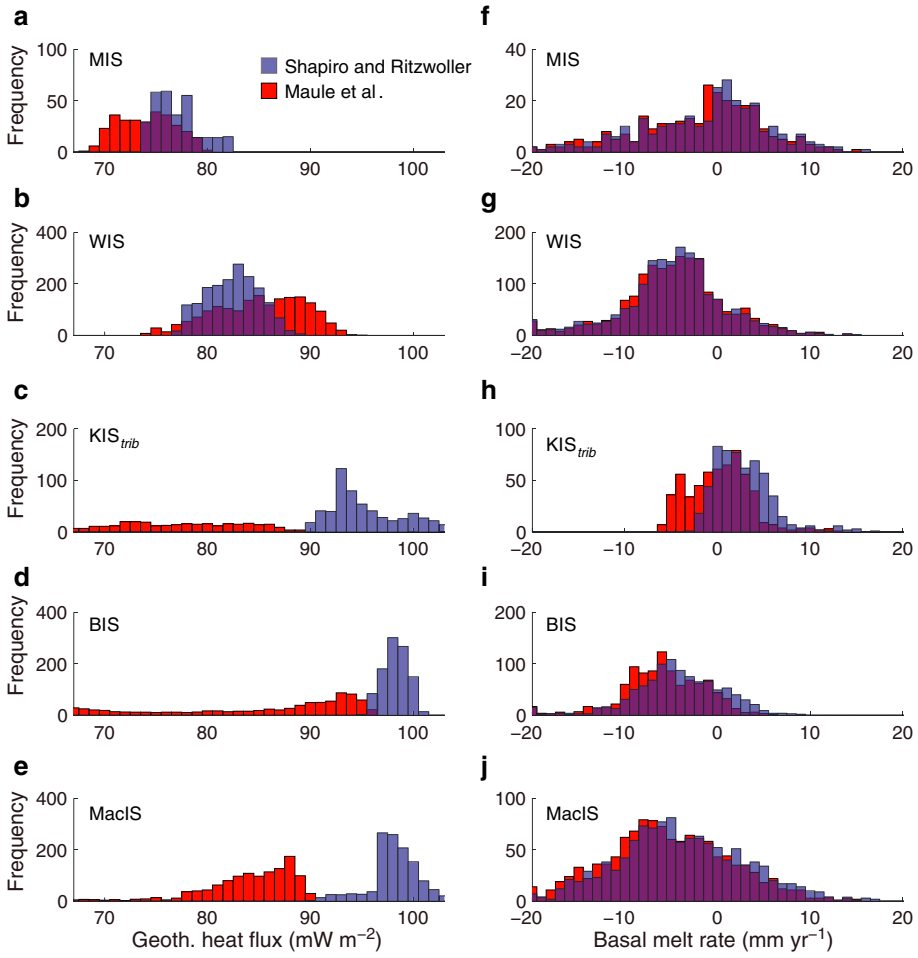

Figure 2. (a–e) Frequency distribution of geothermal heat flux for MIS, WIS, KIS$_{trib}$, BIS, and MacIS. Blue bars represent data from *Shapiro and Ritzwoller* [2004], and red bars show data from *Maule et al.* [2005]. (f–j) Modeled basal melt rates when geothermal heat flux is from Shapiro and Ritzwoller (blue bars) and Maule et al. (red bars).

The geothermal heat flux, however, is more uncertain. We thus conduct our analysis using two different data sets: one with geothermal heat flux values inferred from a global seismic model [*Shapiro and Ritzwoller*, 2004] and another based on magnetic anomalies [*Maule et al.*, 2005]. Despite considerable differences in the estimated geothermal heat flux (Figure 2a), we obtain very similar distributions of basal melting and freezing (Figure 2b). This shows how the geothermal heat flux uncertainty is compensated by frictional heating. The only region where the geothermal heat flux uncertainty appears to significantly influence modeled rates of basal melting is KIS$_{trib}$, but these tributaries form a relatively small part of the investigated area (12%) as well as the total regional meltwater production (Table 1). Therefore, the uncertainty does not significantly influence our overall results.

In the forthcoming analysis, we use the seismically inferred geothermal heat flux data because these feature high values ($>$100 mW m^{-2}) in the tributaries of BIS and MacIS (Figure S1), a region where ice core studies indicate high geothermal heat flow [*Fudge et al.*, 2013]. A robust outcome of our model is that freezing outweighs melting beneath all ice streams (Figure 1b). This outcome is consistent with the observation of 15 m thick accreted basal ice layer in KIS [*Christoffersen et al.*, 2010] and a similar layer in BIS [*Engelhardt*, 2004]. We note, however, that it differs from a previous study, which indicated localized high melt rates beneath BIS and MacIS [*Joughin et al.*, 2004]. The latter are largely absent in our model outputs, but we attribute the difference to the higher-order stresses included in our model as well as our use of Bedmap2, which features more accurate bed topography and ice thickness compared to its predecessor, specifically in the region containing BIS and MacIS (Figure S2).

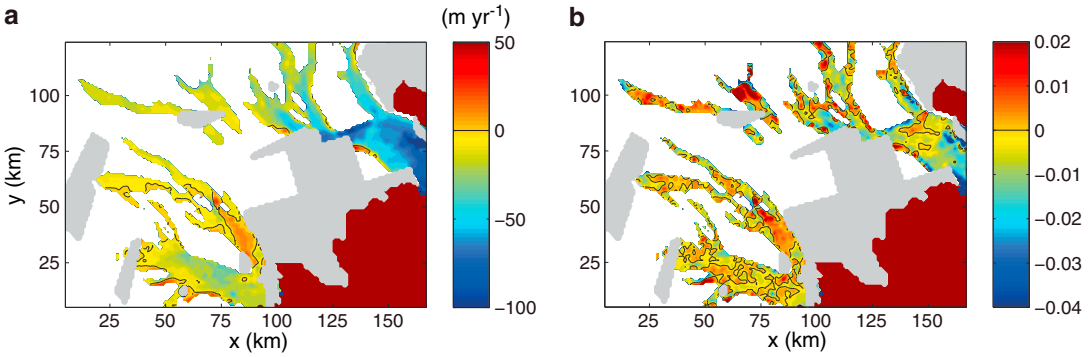

Figure 3. Changes between 1997 and 2009. (a) Change in surface velocities (m yr^{-1}) with positive (negative) numbers denoting an increase (decrease) in speed. (b) Change in till void ratios (dimensionless), with increase (decrease) corresponding to expansion (compaction) of pore space due to inflow (out flow) of water. Areas where surface velocity was measured in 2009 but not in 1997 are shown in grey. Solid black lines show zero contours, and dark red area is the Ross Ice Shelf where ice is afloat. Axes (*x*,*y*) show distance (km) in a polar stereographic grid with reference to 76.727°S and 141.53°W.

3.2. Flow of Water Into and Out of the Till Layer

There are no previous estimates of the annual volumes of water flowing into and out of the till layer beneath the ice streams, although such fluxes have the potential to be a significant part of the regional hydrologic balance. We address this shortcoming by converting basal traction values from the two model inversions into maps of till shear strength and till void ratio. When 2009 velocity data are used in our model, we find that void ratios average 0.57, 0.60, 0.56, and 0.51 in the till beneath the trunks of MIS, WIS, BIS, and MacIS (Figure 1c). The void ratios of till beneath the tributaries (0.44–0.48) are 12–20% lower, indicating stronger till there than beneath the trunks.

A comparison of the two model inversions demonstrates how changes in ice flow (Figure 3a) have occurred in response to physical changes at the bed (Figure 3b). At the trunks of MIS and WIS, basal traction increased by 14% and 22% on average. This basal strengthening was a result of substantial till consolidation. Till void ratios decreased by up to 0.02 at MIS and by up to 0.08 at WIS. Till void ratios also decreased in the tributaries, where basal strengthening amounted to 7% (MIS) and 9% (WIS). Our study therefore demonstrates that the reported slowdown of MIS and WIS [*Joughin et al.*, 2005] is caused by significant till strengthening, an outcome supported by independent force balance analysis of GPS data collected on WIS [*Beem et al.*, 2014].

In order to estimate the annual volume of water entering or leaving the till beneath each ice stream, we need to first estimate the till layer thickness. The latter requires seismic data, which are spatially limited, so we assume for simplicity that till thickness has a normal distribution, with a range bound by end-member values reported in previous studies (i.e., from nil [*Rooney et al.*, 1987] and up to 20 m [*Peters et al.*, 2006]). This yields a characteristic till layer with a mean thickness of 10 m and a standard deviation of 3 m. To estimate the flow of water into and out of the till layer, we combine this till thickness (10 ± 3 m) with the detected till void ratio change. The assumed vertically uniform distribution of till void ratios is consistent with such distribution to a depth of at least 3 m into the till layer at WIS [*Tulaczyk et al.*, 2001]. In this manner, we estimate net outflows of till pore water at MIS (0.02 ± 0.006 km^3 yr^{-1}) as well as WIS (0.26 ± 0.08 km^3 yr^{-1}) (Table 1), whereas there is a net inflow of water to the till layer at KIS_{trib} (-0.02 ± 0.006 km^3 yr^{-1}) (Table 1).

We find entirely different basal conditions at BIS and MacIS. At BIS, inflow of water to the till layer approximately balances the outflow, even though high rates of basal freezing yield -0.11 km^3 yr^{-1} in the hydrologic budget (Table 1). A net reduction in till void ratios at MacIS indicates outflow of till pore water corresponding to 0.02 ± 0.004 km^3 yr^{-1}. The associated till compaction is equivalent to a 2% increase in basal traction, which may explain why surface velocity on this ice stream decreased by up to 46 m yr^{-1} between 1997 and 2009 (Figure 3a). Although the change at MacIS resembles those at MIS and WIS, outflow of pore water from the till layer cannot explain the estimated net loss of water due to high rates of freezing (Table 1).

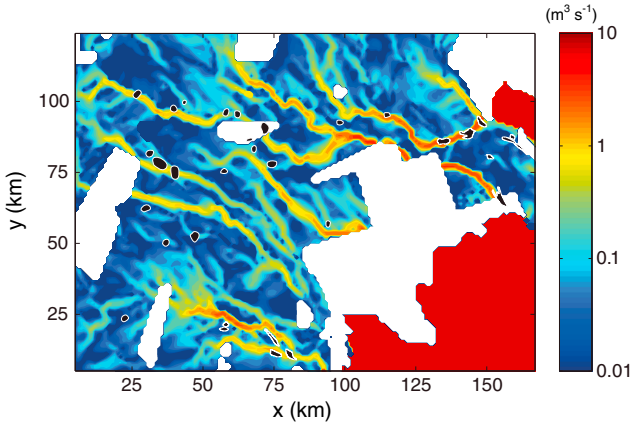

Figure 4. Flow paths and fluxes of water ($m^3\,s^{-1}$ per $5 \times 5\,km^2$ grid cell), when water at the ice-till interface is routed between sources and sinks in hydrologic model. Sources are regions where basal water production is greater than the flow of water into till or where basal freezing is less than flow of water out of till. Sinks are regions where basal water production is less than the flow of water into till or where basal freezing is greater than the flow of water out of till. Major flow paths coincide with observed locations of subglacial lakes, shown in black. Areas not covered by surface velocity data from 1997 are shown in white. Axes (*x*,*y*) show distance (km) in a polar stereographic grid with reference to 76.727°S and 141.53°W.

3.3. Flow of Water Along the Ice-Till Interface

In contrast to previous hydrologic studies in which water was routed according to modeled rates of basal melting and freezing [*Carter and Fricker*, 2012; *Carter et al.*, 2013; *Le Brocq et al.*, 2009], we also route pore water rejected from the till (Table 1). The hydrologic experiment reveals anastomosing channels and anabranches within the subglacial catchment of each ice stream, and major flow paths coincide with observed networks of interconnected subglacial lakes (Figure 4). Water is routed from KIS_{trib} to WIS, consistent with observed connectivity of subglacial lakes in this region [*Carter et al.*, 2013]. The modeled fluxes also indicate outflow of water across the grounding lines. At MIS and WIS, these outflows amount to 0.12 and $0.43\,km^3\,yr^{-1}$. This is more than twice the outflow from BIS ($0.09\,km^3\,yr^{-1}$) and MacIS ($0.10\,km^3\,yr^{-1}$), largely because of the till layer's pore water contribution (Table 1). Because the surface velocity data used in our inversions do not include the entire drainage basins of the ice streams, inflow of water from farther inland is needed to close the hydrologic budgets. According to our model, local sources account for only 28% of the total hydrologic input to BIS and MacIS (Table 1). The remaining 72% is assumed to come from the ice sheet interior. For MIS, WIS, and KIS_{trib}, local sources account for 53% of all inputs, while 47% comes from the ice sheet interior (Table 1).

4. Discussion and Conclusions

Whether ice streams are primarily influenced by till mechanics or subglacial hydrology has been vigorously debated, with paucity of data with which to test hypotheses leading to contrasting models and views [*Alley*, 1996; *Tulaczyk et al.*, 2000b; *Robel et al.*, 2013]. By quantifying hydrologic budgets, our study helps resolve this debate. Of the total hydrologic inputs to MIS, WIS, and KIS_{trib} ($0.98\,km^3\,yr^{-1}$), 47% is inflow of water from the ice sheet interior, while 45% comes from depletion of groundwater and only 8% from local basal ice melting (Table 1). The largest net effects, however, come from basal freezing, which far surpasses basal melting, and the depletion of the groundwater reservoir, which significantly exceeds its recharge (Table 1). Flow of water into the basal water system is countered by outflow at the grounding line. This confirms strong ice-till interactions, as previously hypothesized [*Tulaczyk et al.*, 2000b], and we conclude that till mechanics exert the primary control on the flow of these ice streams. For BIS and MacIS, we estimate hydrologic inputs to amount to $0.56\,km^3\,yr^{-1}$, with the till layer contributing 19%, while local basal ice melting and inflow of water from the ice sheet interior contribute 9% and 72%, respectively. There, the strong offset between basal freezing and melting is countered primarily by a strong offset between inflow to and outflow from the basal water system, while groundwater depletion is roughly balanced by recharge (Table 1). Hence, we conclude that these ice streams are strongly influenced by water transported to them from the ice sheet interior via a regional and through-going basal water system. The subdued response of the till layer beneath BIS and MacIS to the high rates of basal freezing there indicates that the basal water system is spatially widespread and thus of the distributed type. It also appears to be continuously fed by water produced near the onset of these ice streams. Although we can only infer this hydrologic source, its presence is consistent with high geothermal heat flux in this region [*Fudge et al.*, 2012; *Fudge et al.*, 2013]. It is also in agreement with observed extensive subglacial storage of water [*Peters et al.*, 2007] and proposed active subglacial volcanism [*Behrendt et al.*, 2004].

The depletion of till pore water at MIS and WIS indicates that a substantial fraction of water flowing in the basal water system there has been previously stored in till. This finding may have important implications for the search for life in subglacial lakes because till pore water in the Siple Coast region has a much higher solute concentration than subglacial meltwater derived by direct melting of basal ice [*Skidmore et al.*, 2010]. The rates of groundwater recharge in our model yield residence times of till pore water on the order of 1000–10,000 years, providing a long period of time for biogeochemical weathering to result in solute enrichment [*Skidmore et al.*, 2010; *Wadham et al.*, 2010]. Due to significant groundwater release predicted by our simulations, water transported in the basal drainage system at MIS, WIS, and KIS_{trib}, including Subglacial Lakes Whillans explored in situ in 2013 (www.wissard.org), may therefore be particularly enriched in dissolved elements and compounds, some of which may serve as nutrients for microbial life. In contrast, water in the basal zone of BIS and MacIS may, according to our model, contain fewer biogeochemical weathering products because less pore water flows out of the till layer there.

Our study highlights potential large benefits from stronger integration of Earth observation data in numerical ice sheet models. Prediction of sea level rise over the coming decades and centuries inevitably relies on these models having the best possible parameterization of the subglacial environment, which dictates the speed at which ice sheets slide over their beds. The results presented here demonstrate that significant changes can take place in this environment over periods as short as 12 years.

Acknowledgments

This work was carried out with support from the Isaac Newton Trust, Cecil H. and Ida M. Green Foundation and Natural Environment Research Council (grant NE/E005950/1 and NE/J005800/1).

The Editor thanks two anonymous reviewers for their assistance in evaluating this paper.

References

Alley, R. B. (1996), Towards a hydrological model for computerized ice-sheet simulations, *Hydrol. Processes*, *10*(4), 649–660.

Arthern, R. J., D. P. Winebrenner, and D. G. Vaughan (2006), Antarctic snow accumulation mapped using polarization of 4.3-cm wavelength microwave emission, *J. Geophys. Res.*, *111*, D06107, doi:10.1029/2004JD005667.

Beem, L. H., S. M. Tulaczyk, M. A. King, M. Bougamont, H. A. Fricker, and P. Christoffersen (2014), Variable deceleration of Whillans Ice Stream, West Antarctica, *J. Geophys. Res. Earth Surf.*, *119*, doi:10.1002/2013JF002958.

Behrendt, J. C., D. D. Blankenship, D. L. Morse, and R. E. Bell (2004), Shallow-source aeromagnetic anomalies observed over the West Antarctic Ice Sheet compared with coincident bed topography from radar ice sounding - new evidence for glacial "removal" of subglacially erupted late Cenozoic rift-related volcanic edifices, *Global Planet. Change*, *42*(1–4), 177–193.

Bindschadler, R. A., et al. (2013), Ice-sheet model sensitivities to environmental forcing and their use in projecting future sea level (the SeaRISE project), *J. Glaciol.*, *59*(214), 195–224.

Blankenship, D. D., C. R. Bentley, S. T. Rooney, and R. B. Alley (1986), Seismic measurements reveal a saturated porous layer beneath an active Antarctic ice stream, *Nature*, *322*(6074), 54–57.

Bougamont, M., S. Price, P. Christoffersen, and A. J. Payne (2011), Dynamic patterns of ice stream flow in a 3-D higher-order ice sheet model with plastic bed and simplified hydrology, *J. Geophys. Res.*, *116*, F04018, doi:10.1029/2011JF002025.

Carter, S. P., and H. A. Fricker (2012), The supply of subglacial meltwater to the grounding line of the Siple Coast, West Antarctica, *Ann. Glaciol.*, *53*(60), 267–280.

Carter, S. P., H. A. Fricker, and M. R. Siegfried (2013), Evidence of rapid subglacial water piracy under Whillans Ice Stream, *J. Glaciol.*, *59*(218), 1147–1162.

Catania, G., C. Hulbe, H. Conway, T. A. Scambos, and C. F. Raymond (2012), Variability in the mass flux of the Ross ice streams, West Antarctica, over the last millennium, *J. Glaciol.*, *58*(210), 741–752.

Christoffersen, P., S. Tulaczyk, and A. Behar (2010), Basal ice sequences in Antarctic ice stream: Exposure of past hydrologic conditions and a principal mode of sediment transfer, *J. Geophys. Res.*, *115*, F03034, doi:10.1029/2009JF001430.

Clarke, G. K. C. (1987), Subglacial till: A physical framework for its properties and processes, *J. Geophys. Res.*, *92*(B9), 9023–9036.

Clarke, G. K. C. (2005), Subglacial processes, *Ann. Rev. Earth Planet Sci.*, *33*, 247–276.

Comiso, J. C. (2000), Variability and trends in Antarctic surface temperatures from in situ and satellite infrared measurements, *J. Clim.*, *13*(10), 1674–1696.

Engelhardt, H. (2004), Thermal regime and dynamics of the West Antarctic ice sheet, *Ann. Glaciol.*, *39*, 85–92.

Engelhardt, H., and B. Kamb (1998), Basal sliding of Ice Stream B, West Antarctica, *J. Glaciol.*, *44*(147), 223–230.

Engelhardt, H., N. Humphrey, B. Kamb, and M. Fahnestock (1990), Physical conditions at the base of a fast moving Antarctic ice stream, *Science*, *248*(4951), 57–59.

Fretwell, P., et al. (2013), Bedmap2: Improved ice bed, surface and thickness datasets for Antarctica, *Cryosphere*, *7*(1), 375–393.

Fricker, H. A., T. Scambos, R. Bindschadler, and L. Padman (2007), An active subglacial water system in West Antarctica mapped from space, *Science*, *315*(5818), 1544–1548.

Fudge, T. J., G. D. Clow, H. Conway, K. Cuffey, M. Koutnik, T. A. Neumann, K. C. Taylor, and E. Waddington (2012), High Basal Melt at the WAIS-Divide ice-core site, *WAIS Workshop 2012*, Eatonville, Wash.

Fudge, T. J., et al. (2013), Onset of deglacial warming in West Antarctica driven by local orbital forcing, *Nature*, *500*(7463), 440–444.

Gray, L., I. Joughin, S. Tulaczyk, V. B. Spikes, R. Bindschadler, and K. Jezek (2005), Evidence for subglacial water transport in the West Antarctic Ice Sheet through three-dimensional satellite radar interferometry, *Geophys. Res. Lett.*, *32*, L03501, doi:10.1029/2004GL021387.

Hooke, R. L., B. Hanson, N. R. Iverson, P. Jansson, and U. H. Fischer (1997), Rheology of till beneath Storglaciaren, Sweden, *J. Glaciology*, *43*(143), 172–179.

Hulbe, C., and M. Fahnestock (2007), Century-scale discharge stagnation and reactivation of the Ross ice streams, West Antarctica, *J. Geophys. Res.*, *112*, F03S27, doi:10.1029/2006JF000603.

Iverson, N. R., T. S. Hooyer, and R. W. Baker (1998), Ring-shear studies of till deformation: Coulomb-plastic behavior and distributed strain in glacier beds, *J. Glaciol.*, *44*(148), 634–642.

Joughin, I., S. Tulaczyk, R. Bindschadler, and S. F. Price (2002), Changes in west Antarctic ice stream velocities: Observation and analysis, *J. Geophys. Res.*, *107*(B11), 2289, doi:10.1029/2001JB001029.

Joughin, I., S. Tulaczyk, D. R. MacAyeal, and H. Engelhardt (2004), Melting and freezing beneath the Ross ice streams, Antarctica, *J. Glaciol.*, *50*(168), 96–108.

Joughin, I., et al. (2005), Continued deceleration of Whillans Ice Stream, West Antarctica, *Geophys. Res. Lett.*, *32*, L22501, doi:10.1029/2005GL024319.

Kamb, B. (1991), Rheological nonlinearity and flow instability in the deforming bed mechanism of ice stream motion, *J. Geophys. Res.*, *96*(B10), 16,585–16,595.

Kamb, B. (2001), Basal zone of the West Antarctic ice streams and its role in lubrication of their rapid motion, in *The West Antarctic Ice Sheet: Behavior and Environment*, Antarctic Research Series, vol. 77, edited by R. B. Alley and R. A. Bindschadler, pp. 157–201, AGU, Washington D. C.

Le Brocq, A. M., A. J. Payne, M. J. Siegert, and R. B. Alley (2009), A subglacial water-flow model for West Antarctica, *J. Glaciol.*, *55*(193), 879–888.

Maule, C. F., M. E. Purucker, N. Olsen, and K. Mosegaard (2005), Heat flux anomalies in Antarctica revealed by satellite magnetic data, *Science*, *309*(5733), 464–467.

Peters, L. E., S. Anandakrishnan, R. B. Alley, and A. M. Smith (2007), Extensive storage of basal meltwater in the onset region of a major West Antarctic ice stream, *Geology*, *35*(3), 251–254.

Peters, L. E., S. Anandakrishnan, R. B. Alley, J. P. Winberry, D. E. Voigt, A. M. Smith, and D. L. Morse (2006), Subglacial sediments as a control on the onset and location of two Siple Coast ice streams, West Antarctica, *J. Geophys. Res.*, *111*, B01302, doi:10.1029/2005JB003766.

Price, S. F., A. J. Payne, I. M. Howat, and B. E. Smith (2011), Committed sea-level rise for the next century from Greenland ice sheet dynamics during the past decade, *Proc. Natl. Acad. Sci. U. S. A.*, *108*(22), 8978–8983.

Rathbun, A. P., C. Marone, R. B. Alley, and S. Anandakrishnan (2008), Laboratory study of the frictional rheology of sheared till, *J. Geophys. Res.*, *113*, F02020, doi:10.1029/2007JF000815.

Rignot, E., J. Mouginot, and B. Scheuchl (2011), Ice Flow of the Antarctic Ice Sheet, *Science*, *333*(6048), 1427–1430.

Rignot, E., J. L. Bamber, M. R. Van Den Broeke, C. Davis, Y. H. Li, W. J. Van De Berg, and E. Van Meijgaard (2008), Recent Antarctic ice mass loss from radar interferometry and regional climate modelling, *Nat. Geosci.*, *1*(2), 106–110.

Robel, A. A., E. DeGiuli, C. Schoof, and E. Tziperman (2013), Dynamics of ice stream temporal variability: Modes, scales, and hysteresis, *J. Geophys. Res. Earth Surf.*, *118*, 925–936, doi:10.1002/jgrf.20072.

Rooney, S. T., D. D. Blankenship, R. B. Alley, and C. R. Bentley (1987), Till beneath Ice Stream-B .2. Structure and continuity, *J. Geophys. Res.*, *92*(B9), 8913–8920.

Shapiro, N. M., and M. H. Ritzwoller (2004), Inferring surface heat flux distributions guided by a global seismic model: Particular application to Antarctica, *Earth Planet. Sci. Lett.*, *223*(1–2), 213–224.

Shepherd, A., et al. (2012), A Reconciled Estimate of Ice-Sheet Mass Balance, *Science*, *338*(6111), 1183–1189.

Skidmore, M., M. Tranter, S. Tulaczyk, and B. Lanoil (2010), Hydrochemistry of ice stream beds - evaporitic or microbial effects?, *Hydrol. Processes*, *24*(4), 517–523.

Smith, A. M. (1997), Basal conditions on Rutford Ice Stream, West Antarctica, from seismic observations, *J. Geophys. Res.*, *102*(B1), 543–552.

Tulaczyk, S., W. B. Kamb, and H. F. Engelhardt (2000a), Basal mechanics of Ice Stream B, West Antarctica 1. Till mechanics, *J. Geophys. Res.*, *105*(B1), 463–481.

Tulaczyk, S., W. B. Kamb, and H. F. Engelhardt (2000b), Basal mechanics of Ice Stream B, West Antarctica 2. Undrained plastic bed model, *J. Geophys. Res.*, *105*(B1), 483–494.

Tulaczyk, S., W. B. Kamb, and H. F. Engelhardt (2001), Estimates of effective stress beneath a modern West Antarctic ice stream from till preconsolidation and void ratio, *Boreas*, *30*, 101–114.

Wadham, J. L., M. Tranter, M. Skidmore, A. J. Hodson, J. Priscu, W. B. Lyons, M. Sharp, P. Wynn, and M. Jackson (2010), Biogeochemical weathering under ice: Size matters, *Global Biogeochem. Cycles*, *24*, GB3025, doi:10.1029/2009GB003688.